低温水热前驱物技术制备单晶 PbS 纳米片

胡寒梅*,[1] 邓崇海[2] 黄显怀[3] 李 燕[1] 孙 梅[1] 张克华[1]
([1]安徽建筑工业学院材料与化学工程学院,合肥 230022)
([2]合肥学院化学与材料工程系,合肥 230022)
([3]安徽建筑工业学院环境工程学院,合肥 230022)

摘要:以层状的铅(Ⅱ)-硫脲配合物为前驱体,在 130 ℃反应 12 h 水热分解得到高产量的半导体单晶 PbS 二维纳米片,产品用 XRD、TEM、SEM、ED、XPS 进行了表征,单晶 PbS 纳米片的二维尺寸为 0.6~3 μm,厚度为 2~4 nm,沿着 *ab* 平面生长。紫外吸收光谱和光致发光光谱表明二维 PbS 纳米片的量子尺寸效应非常显著。对可能的生长机理进行了探讨。

关键词:硫化铅;水热技术;前驱体;纳米片
中图分类号:O611.4;O613.5 **文献标识码**:A **文章编号**:1001-4861(2007)04-1403-06

Hydrothermal Precursor Approach to Single-crystal PbS Nanosheets at Low Temperature

HU Han-Mei*,[1] DENG Chong-Hai[2] Huang Xian-Huai[3] LI Yan[1] SUN Mei[1] ZHANG Ke-Hua[1]
([1]*Department of Materials and Chemical Engineering, Anhui Institute Architecture & Industry, Hefei* 230022)
([2]*Department of Chemistry and Materials Engineering, Hefei University, Hefei* 230022)
([3]*Department of Environment Engineering, Anhui Institute Architecture & Industry, Hefei* 230022)

Abstract: Semiconductor PbS single-crystal nanosheets with micrometer-scale lateral dimensions have been synthesized on a large scale by hydrothermal decomposition of the lamellar precursor-Pb(Ⅱ)-thiourea complexes at a low temperature of 130 ℃ for 12 h. XRD, TEM, SEM, electron diffraction (ED) and XPS were used to characterize the final product. The products are sheet-like with rectangle lateral dimensions in the range of 0.6~3 μm and thickness of 2~4 nm which grow along the a and b axes two-dimensional (2D) direction simultaneously. UV-Vis absorption and Photoluminescence (PL) spectra reveal that the as-prepared products have shown considerably greater quantum size effects expected for the 2D ultrathin nanostructure. The possible formation mechanism has been proposed.

Key words: PbS; hydrothermal technique; precursor; nanosheet

0 Introduction

One-dimentional (1D) nanostructured materials, such as nanorods, nanowires or nanotubes, have been successfully synthesized and have received much attention due to their peculiar optical, electrical, thermoelectric properties and potential applications in nanodevices[1~3]. Two-dimensional (2D) nanostructure such as nanosheets is also an important category of nanostructured materials to which increasing attention has been paid recently[4,5]. As a new class of nanosized semiconductors, nanosheet materials are characterized

收稿日期:2007-04-18。收修改稿日期:2007-05-31。
国家自然科学基金(No.20501002),安徽省教育厅自然科学基金(No.2005KJ110,2006KJ159B),安徽省高校青年教师科研资助计划项目(No.2005jq1147zd,2006jq1228),安徽建筑工业学院博士启动基金(No.2004002)资助。
*通讯联系人。E-mail:hmhu@ustc.edu
第一作者:胡寒梅,女,31 岁,博士,副教授;研究方向:无机纳米材料的合成和性能研究。

by high crystallinity and well-defined chemical composition as well as extremely high anisotropy with an ultra thin thickness. These unusual features will result in distinctive physicochemical properties in comparison with conventional nanocrystals mostly in spherical shape. The nanosheet crystals of $Ti_{1-\delta}O_2^{4\delta-}$ (δ ~0.09) show very sharp optical absorption peak which is considerably blue-shifted relative to the band gap energy of bulk titanium oxides[6]. Ga_2O_3 nanobelts, nanoribbons and nanosheets were obtained by various methods[7~9]. Metal platinum nanosheets containing hexagonal holes were formed between graphite layers by hydrogen reduction of platinum chloride-graphite intercalation compounds[10]. Wurtzite ZnS single-crystal nanosheets can be generated by thermal decomposition of the lamellar precursor in vacuum at 250 ℃[11]. Generally, High temperature and vacuum or template are needed in preparing these 2D nanocrystals.

As an important Ⅳ-Ⅵ group material, PbS has attracted considerable attention due to its small band gap energy (0.41 eV) and large exciton Bohr radius (18 nm), which allows for the strong quantum confinement with relatively large nanocrystals [12]. Consequently, obtaining PbS nanocrytals with special morphology is potentially meaningful in finding novel applications of such kinds of semiconductors. To the best of our knowledge, controlling growth of 2D PbS nanostructure has not been reported up to now although there are some reports on the preparation of PbS with different morphologies, such as uniform cubic-shaped nanocrystals[13], nanorods[14], nanowires[15], star-shaped[16], hierarchical nanostructures[17], nanotubes [18], hollow nanospheres[19] etc.

Herein, we report the synthesis of PbS nanosheets in large quantities with well crystalliztion by a mild hydrothermal decomposition of single-source precursor-Pb (Ⅱ)-thiourea complexes at low temperature. Under such conditions, toxic solvents such as ethylenediamine, pyridine and benzene can be avoided. Desired morphologies of materials with excellent optical properties have been obtained. A possible formation mechanism of nanosheets was proposed. This method is favorable for green environmental protection without use of any toxicant organic solvents and surfactants.

1 Experimental

Preparation of single-source precursor-Pb(Ⅱ)-thiourea complexes: Analytical grade purity (A.R.) $Pb(NO_3)_2$ and $SC(NH_2)_2$ were purchased from Sinopharm Chemical Reagent Co. Ltd. In a typical procedure, $Pb(NO_3)_2$ and $SC(NH_2)_2$ with a molar ratio of 1∶2 were used as starting materials. At first, $Pb(NO_3)_2$ was dissolved in a small amount of distilled water in order to improve its solubility. Then the obtained solution was mixed with a solution of thiourea in 60 mL ethanol. After stirring for 3~4 days at 60 ℃, the solution was filtered and a gray-color crystalline solid obtained. The solid was washed with absolute ethanol several times, and then dried in vacuum at 60 ℃ for 8 h.

Preparation of PbS single-crystal nanosheets: 0.25 g single-source precursor was loaded into a 50 mL Telfon-lined stainless steel autoclave, which was then filled with distilled water up to 90% of the total volume. The sealed autoclave was maintained at 130 ℃ for 12 h, cooled to room temperature naturally. The flake-like products with metallic light-gray color and high reflective luster were collected by vacuum filtration, washed with absolute ethanol and distilled water several times to remove the impurities, then dried in vacuum at 60 ℃ for 8 h before further characterization.

The obtained single-source precursor was characterized by FTIR spectroscopy operating on a Bruker Vector-22FTIR spectrophotometer with KBr pellets in the 4 000~400 cm^{-1} region. The final products were determined by XRD using a Japan Rigaku D/max r-A X-ray diffractometer with graphite monochromatized Cu $K\alpha$ radiation (λ =0.154 06 nm). The morphology and size of as-prepared products were observed by TEM and SEM images, which were performed on a Hitachi model H-800 and an X-650 scanning electronic microanalyzer, respectively. XPS spectra were recorded on a VGESCALAB MKII X-ray photoelectron spectrometer, using a non-monchromatized Mg $K\alpha$ X-ray as the excitation source to investigate the surface

constituents. The binding energy data were calibrated with reference to C1*s* (284.5 eV). UV-Vis absorption spectrum was recorded on a Shimadzu UV-2100 spectrophotometer with ethanol as the reference. Photoluminescence (PL) spectrum was carried out on a Hitachi 850 fluorescence spectrophotometer.

2 Results and discussion

2.1 FTIR spectra of the single-source precursor

In the FTIR spectrum of the single-source precursor, there are three characteristic absorption peaks of the -NH_2 stretching vibration of Pb(Ⅱ)-thiourea complexes at 3 404, 3 300 and 3 195 cm^{-1}, which do not shift to lower frequencies on the formation of the metal-thiourea complexes[20,21]. It is suggested that nitro gen-to-metal bond is not present. Comparing with the FTIR spectrum of pure thiourea, the frequency of the C-N stretching vibration is blue-shifted from 1 473 cm^{-1} to 1 525 cm^{-1} due to the greater double bond character of the C-N bond on complex formation; and the frequency of the C=S stretching vibration is red-shifted from 730 cm^{-1} to 694 cm^{-1} attributed to the reduced double bond character of C=S bond. Meanwhile, a strong absorption of thiourea at 1 083 cm^{-1} disappears on the complex formation. In addition, the two strong bands at 1 383 cm^{-1} and 817 cm^{-1} are assigned to the nitrate ion[22,23]. A conclusion can be drawn that the thiourea uses sulfur atom to coordinate with metal Pb(Ⅱ) cation.

2.2 Characterization of the as-prepared products

The XRD pattern of the sample is shown in Fig. 1. All the diffraction peaks can be indexed to face-centered cubic phase PbS with calculated cell constant a=0.593 9 nm, which is in agreement with the literature datum a=0.593 6 nm (PDF2 05-0592). No evidence of other impurities can be detected in the pattern. The intense diffraction peaks suggest that the sample be well crystallized. The (200) and (400) reflections are relatively strong compared with the standard stick pattern for bulk PbS, indicating that the obtained sheet-like PbS product probably have a preferential growing facet.

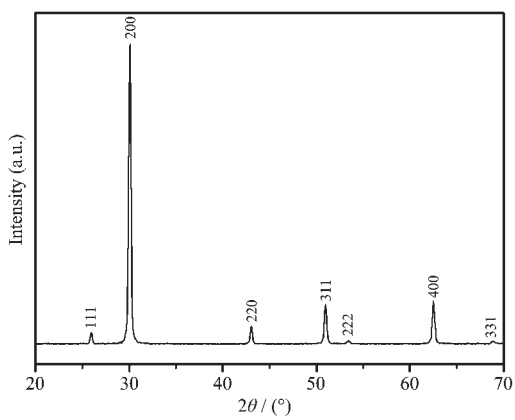

Fig.1　XRD pattern of the as-prepared products

Fig.2 gives the XPS spectra of the sample. A typical survey spectrum of PbS is shown in Fig.2a. The peaks of Pb and S can be clearly detected as well as those of C and O, which are attributed to the gaseous molecules from the air absorbed on the surfaces of the products. Fig.2b and 2c reveal the photoelectron spectrum of Pb4*f* core level and S2*p* core level, respectively. The peaks at 137.10 eV and 142.15 eV correspond to the binding energy of Pb4$f_{7/2}$ and Pb4$f_{5/2}$. Meanwhile, the corresponding binding

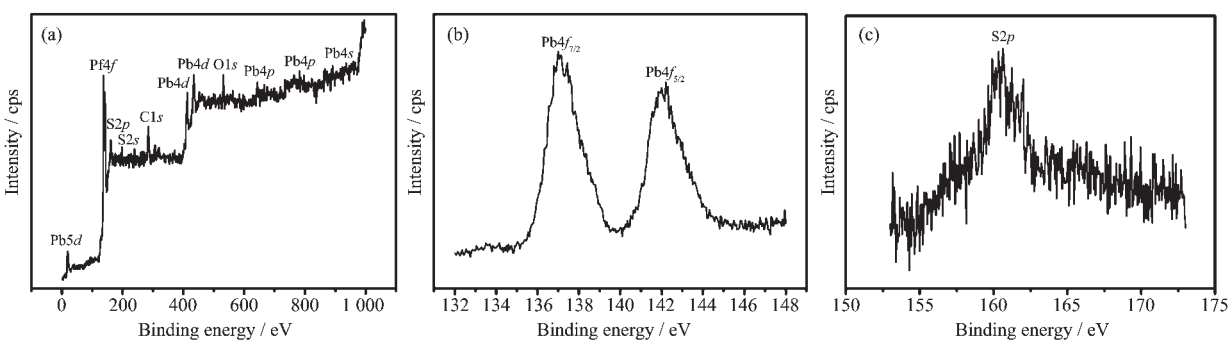

(a) typical survey spectrum; (b) Pb4*f* core level; (c) S2*p* core level

Fig.2　XPS spectra of the as-prepared products

energy of S2*p* is 160.10 eV. After quantitative calculation from the peak areas of Pb4*f* and S2*p*, they give the molar ratio of the product as 0.951∶1.000 for Pb∶S. The result is in good agreement with the given formula for the as-prepared product.

Surface topographies of the as-prepared products are shown in Fig.3. TEM images (Fig.3a, 3b) clearly show that the PbS nanoparticles are sheet-like with rectangle lateral dimensions in the range of 0.6 ~3 μm. The selected area electron diffraction (SAED) patterns (Fig.3c) from one nanosheet crystallite display a cubic array of sharp spots, which indicates single-crystal quality as well as the high crystallinity of the PbS nanosheets. Two typical diffraction spots can be indexed as the (200) and (220) lattice planes, respectively, which are similar to the diffraction peaks indexed in the XRD pattern and the zone axis is [001]. It is suggested that the surface of the nanosheets should be (002) lattice plane and the nanosheets of as-prepared PbS grow along the a and b axes in two-dimensional (2D) direction simultaneously. SEM image (Fig.3d) shows that quantities of single-layer nanosheets are self-assembled together to multiple layered structures via weaker Vannder Waals interaction. This phenomenon can be attributed to comparatively higher surface areas and higher surface energies of the ultra thin nanosheets. Based on TEM and SEM results, the thickness of PbS nanosheets is estimated to be 2~4 nm.

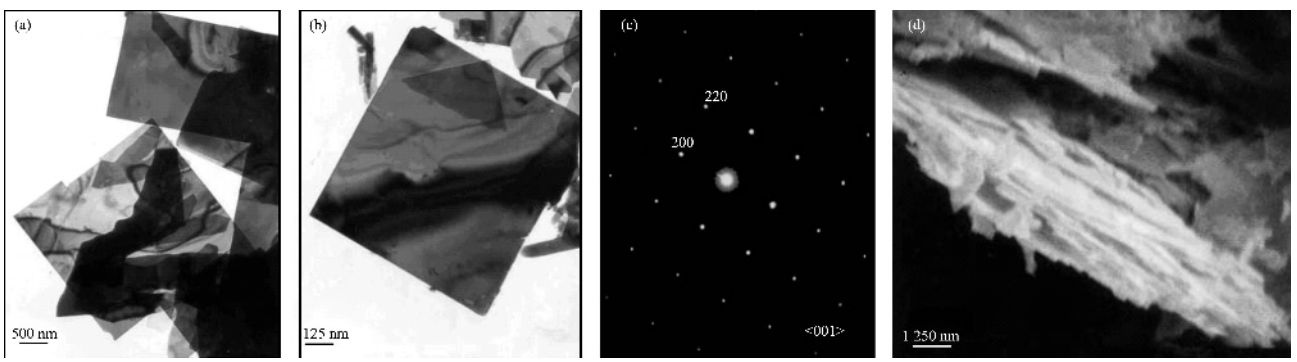

Fig.3 (a, b) TEM images of the as-prepared products; (c) ED pattern of the as-prepared products; (d) SEM images of the as-prepared products

2.3 Optical properties

The photoelectrochemistry of small semiconductor particles has been an area of active research. Of particular interest is their property of photoinduced blue shifts in the absorption spectra[24]. Bulk PbS has a very small direct band gap of 0.41 eV at 298 K, with an absorption onset at 3 020 nm. When the crystallite size is reduced to the nanometer size range, the absorption edge of PbS will exhibit a large blue-shift under photoinduction. The origin of the blue-shift has been attributed to the quantum confinement of charge carriers in the nanoparticles[25]. The absorption spectrum of the sample is shown in Fig.4a. Three excitonic peaks at 225 nm (5.52 eV), 280 nm (4.44

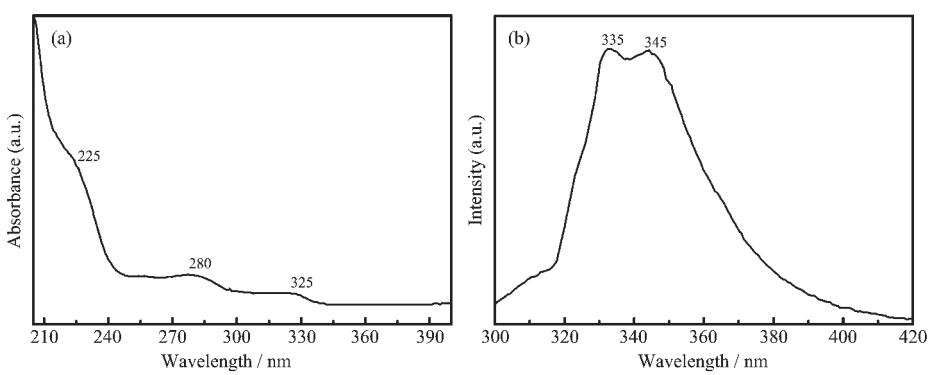

Fig.4 (a) UV-Vis absorption spectrum of PbS nanosheets; (b) Photoluminescence spectrum of PbS nanosheets

eV) and 325 nm (3.82 eV) are apparently observed. The presence of excitonic effects can be due to the carrier confinement produced through the correlation between the confined electron and hole[26]. The large blue shift results from quantum size effects of the PbS 2D nanosheets. The photoluminescence (PL) spectrum of the sample is given in Fig.4b. The spectrum shows a sharp emission peak at 335 nm and a shoulder peak at 345 nm (λ_{ex}=235 nm). Other study is worth to be noticed that PbS colloids with D_p ~2 nm show two emission peaks at 436 and 600 nm[27]. In the present case, the marked blue shift of the emission band position may be due to the utra thin nature of the as-prepared nanosheets, and it may have potential applications for the photoelectrochemistry.

2.4 Reaction mechanism

In the present case of the formation of PbS nanosheets, we believe that there are several kinds of affecting factors. First, the flake-like precursor originated from lead salts and thiourea may act as a structure-directing agent for the maintenance of lamellar shape (Fig.5a). If using $Pb(NO_3)_2$ and $SC(NH_2)_2$ rather than Pb (Ⅱ)-thiourea complexes as stating materials, keeping other conditions unchanged, dendrite-shaped PbS crystals and a small amount of nanosheets are obtained (Fig.5b). It is suggested that the preparation of the flake-like precursor in advance is helpful for the obtainment of PbS nanosheets. Second, solvent water plays an important assistant role in the formation of nanosheets. The precursor can be easily dispersed in water under stirring, forming a homo-geneous solution which is beneficial for homogeneous nucleation. The effects of hydrogen bonds between -NH_2 in thiourea and -OH in water should be considered. A 2D network array may be formed through the action of the hydrogen bonds, which acts as a "soft template", leading to the growth of PbS nuclei into nanosheets. The explanation can be proved by further experiment. If using solvent containing hydroxyl groups such as ethanol, the as-product can be obtained as well as some small cube-shape nanocrystals (Fig.5c). These cubic crystals may result from the poor solubility of the precursor in ethanol. The amount of "soft template" is small before the beginning of hydrothermal decom-position. In the present experimental system, hetero-geneous system is

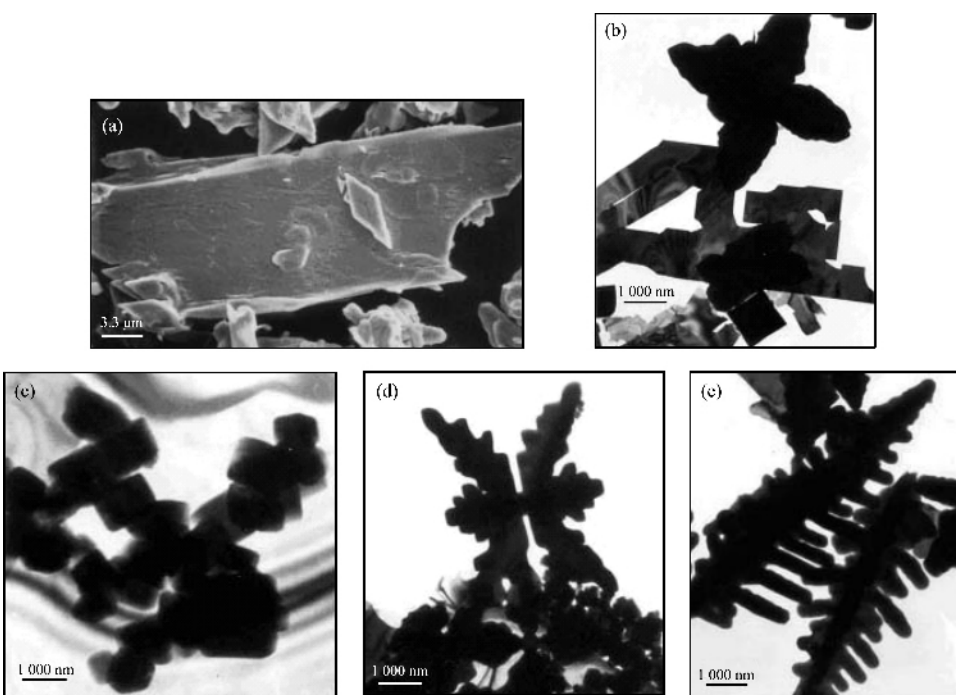

Fig.5 (a) SEM image of the single-source precursor; (b) TEM image of solvothermal reaction using $Pb(NO_3)_2$ and $SC(NH_2)_2$; (c) TEM image of solvothermal reaction in ethanol at 130 ℃ for 12 h; (d) TEM image of solvothermal reaction in ethyenediamine at 130℃ for 12 h; (e) TEM image of hydrothermal reaction in water at 150 ℃ for 12 h

unfavorable for the formation of the as-desired product. While taking nucleophilic polar solvent ethyenediamine instead of water, cubic particles, nanosheets and symmetrical flake-like dendrites can be interestingly found (Fig.5d). These experiments indicate that different solvents have different effects on the precursor and further affect the process of hydrothermal decomposition and ultimately influence the morphologies of the final product. Third, temperature is another critical factor for the growth of PbS nanosheets. Low temperature (120~130 ℃) is beneficial for the formation of nanosheets. When the temperature is increased to 150 ℃, dendrite-like particles will appear (Fig.5e). The appearance of den-drites should be explained that the precursor quickly decomposes at comparatively higher temperature, a certain critical supersaturation concentration is attained, and a dendritic array is expected to appear[28]. Our present understanding of the mechanism for the formation of the PbS nanosheets is still limited, and more in-depth studies are still needed.

3 Conclusions

2D semiconductor PbS single-crystal nanosheets with high yield (95%) have been synthesized by hydrothermal decomposition of the lamellar precursor-Pb (Ⅱ)-thiourea complexes at lower temperature. UV-Vis absorption and PL spectra reveal that the as-prepared PbS nanosheets have considerably greater quantum size effects due to the ultra thin nature of the nanosheets. The parallel experiments suggest that lamellar precursor is benificial to the formation of two-dimensional nanoparticles.

References:

[1] Ajayan P M. *Chem. Rev.*, **1999**,**99**:1787~1799

[2] Duan X F, Huang Y, Cui Y, et al. *Nature*, **2001**,**409**:66~69

[3] Peng Z A, Peng X G. *J. Am. Chem. Soc.*, **2001**,**123**:183~184

[4] Shirai M, Igeta K, Arai M. *J. Phy. Chem. B*, **2001**,**105**:7211~7215

[5] Miyamoto N, Yamamoto H, Kaito R, et al. *Chem. Commun.*, **2002**,**20**:2378~2379

[6] Sasaki T, Watanabe M. *J. Phys. Chem. B*, **1997**,**101**:10159~10161

[7] Dai L, Chen X L, Zhang X N, et al. *J. Appl. Phys.*, **2002**,**92**:1062~1065

[8] Dai Z R, Pan Z W, Wang Z L. *J. Phys. Chem. B*, **2002**,**106**:902~904

[9] Gundiah G, Govindaraj A, Rao C N R. *Chem. Phys. Lett.*, **2002**,**351**:189~194

[10]Shirai M, Igeta K, Arai M. *Chem. Comm.*, **2000**,**7**:623~624

[11]Yu S H, Yoshimura M. *Adv. Mater.*, **2002**,**14**:296~300

[12]Krauss T D, Wise F W. *Phys. Rev. B*, **1997**,**55**:9860~9865

[13]Jiang Y, Wu Y, Xie B, et al. *J. Crystal Growth*, **2001**,**231**:248~251

[14]Wan J X, Chen X Y, Wang Z H, et al. *Mater. Chem. Phys.*, **2004**,**88**:217~220

[15]Yu D B, Wang D B, Meng Z Y, et al. *J. Mater. Chem.*, **2002**,**12**:403~405

[16]Lee S M, Jun Y W, Cho S N, et al. *J. Am. Chem. Soc.*, **2002**,**124**:11244~11245

[17]Ma Y R, Qi L M, Ma J M, et al. *Cryst. Growth Des.*, **2004**,**4**:351~354

[18]Zhang C, Kang Z, Shen E, et al. *J. Phys. Chem. B*, **2006**,**110**:184~189

[19]Wang S F, Gu F, Lu M K. *Langmuir*, **2006**,**22**:398~401

[20]Yamaguchi A, Penland R B, Mizushima S, et al. *J. Am. Chem. Soc.*, **1958**,**80**:527~529

[21]Yang J, Zeng J H, Yu S H, et al. *Chem. Mater.*, **2000**,**12**:2924~2929

[22]Silverstein R M, Bassler G C, Morrill T C. *Spectrometric Identification of Organic Compounds*. New York: Wiley, **1981**.107

[23]Nakamoto K. *Infrared Spectra of Coordination Compounds*. New York: Wiley, **1970**.171

[24]Kowshik M, Vogel W, Urban J, et al. *Adv. Mater.*, **2002**,**14**:815~818

[25]Brus L. *J. Phys. Chem.*, **1986**,**90**:2555~2560

[26]Brus L E. *J. Chem. Phys.*, **1984**,**80**:4403~4405

[27]Nozik A J, Williams F, Nenadovic M T, et al. *J. Phys. Chem.*, **1985**,**89**:397~399

[28]Sunagawa I. *Bull. Mineral*, **1981**,**104**:81~87